Advances in Computational & Experimental Engineering & Science

Microscopic Bifurcation and Post-Bifurcation Behavior of Periodic Cellular Solids

N. Ohno[1], D. Okumura[1], H. Noguchi[2]

Summary

A general framework to analyze microscopic bifurcation and post-bifurcation behavior of elastoplastic, periodic cellular solids is developed on the basis of a two-scale theory of the updated Lagrangian type. We thus derive the eigenmode problem of microscopic bifurcation and the orthogonality to be satisfied by the eigenmodes. By use of the framework, then, bifurcation and post-bifurcation analysis are performed for cell aggregates of an elastoplastic honeycomb subject to in-plane compression. Thus, demonstrating a long-wave eigenmode of microscopic bifurcation under uniaxial compression, it is shown that the eigenmode causes microscopic buckling to localize in a cell row perpendicular to the loading axis. It is also shown that under equi-biaxial compression, the flower-like buckling mode having occurred in a macroscopically stable state changes into an asymmetric, long-wave mode due to the sextuple bifurcation in a macroscopically unstable state, leading to the localization of microscopic buckling in deltaic areas.

Introduction

When cellular solids are subject to compression, buckling may occur in cell walls and edges. This kind of buckling, which is called microscopic buckling, is of interest from a mechanics point of view because of two features: The first is the complexity of buckling modes, which has been typically observed in hexagonal honeycombs [1, 2]. The second is the macroscopic localization of microscopic buckling. When metallic and polymer honeycombs were transversely compressed, microscopic buckling was likely to localize in a cell row and then propagate to the neighboring cell rows, yet it localized rather broadly under equi-biaxial compression [2]. Such macroscopic localization may be enhanced by microscopic plastic deformation, since it generally greatly reduces macroscopic stiffness.

In this study, a general framework to analyze microscopic bifurcation and post-bifurcation behavior of elastoplastic, periodic cellular solids is built on the basis of the updated Lagrangian type of two-scale theory developed in [3]. By use of the framework, bifurcation and post-bifurcation analysis are performed for cell aggregates of an elastoplastic honeycomb subject to in-plane compression.

Theory

We consider an infinite, periodic body $\mathcal{B}$ that has a unit cell Y and is subject to macroscopically uniform stress or strain. A general framework is then established by

[1] Department of Mechanical Engineering, Nagoya University, Chikusa-ku, Nagoya 464-8603, Japan
[2] Department of System Design Engineering, Keio University, Kohoku-ku, Yokohama 223-8522, Japan

Proceedings of the 2004 International Conference on Computational & Experimental Engineering & Science
26-29 July, 2004, Madeira, Portugal

employing a two-scale theory of the updated Lagrangian type and by taking into account the *kY*-periodicity of microscopic deformation as well as the multiplicity of microscopic bifurcation. Here, *kY* indicates a cell aggregate consisting of *k* unit cells. The framework is generally built without recourse to the symmetry of microscopic bifurcation in contrast to the previous framework [3]. Velocity $\dot{u}_i$ is decomposed into macroscopic part $\dot{u}_i^0$ and microscopic, *kY*-periodic part $\dot{u}_i^*$. We thus derive the eigenmode problem of microscopic bifurcation, Eq. (1), and the orthogonality to be satisfied by the eingenmodes, Eq. (2):

$$\left\langle l_{ijkl}\phi_{k,l}^{(r)}\delta\dot{u}_{i,j}^{*}\right\rangle = 0\,, \quad r = 1, 2, \ldots, m\,, \tag{1}$$

$$\left\langle l_{ijkl}\phi_{k,l}^{(r)}\right\rangle = 0\,, \quad r = 1, 2, \ldots, m\,, \tag{2}$$

where $\langle\ \rangle$ indicates the volume average in *kY*, l_{ijkl} expresses microscopic stiffness, $\phi_i^{(r)}$ $(r = 1,\ 2,\ \ldots, m)$ denote eigenmodes, $\delta\dot{u}_i^*$ is any *kY*-periodic velocity field, $(\ )_{,i}$ represents the differentiation with respect to Cartesian coordinate x_i, and m signifies the degree of multiplicity.

Eq. (1) holds with respect to any *kY*-periodic velocity field $\delta\dot{u}_i^*$. Hence, taking $\delta\dot{u}_i^* = \phi_i^{(s)}$ in (1), we have $\left\langle l_{ijkl}\phi_{i,j}^{(r)}\phi_{k,l}^{(s)}\right\rangle = 0$, $r = 1, 2, \ldots, m$, $s = 1, 2, \ldots, m$. Consequently, if microscopic bifurcation occurs, the stability condition of Hill is interrupted.

We can show that at the onset of microscopic bifurcation, orthogonality (2) allows the macroscopic increments to be determined independently of the eigenmodes, resulting in a simple procedure of the elastoplastic post-bifurcation analysis based on the notion of comparison solids.

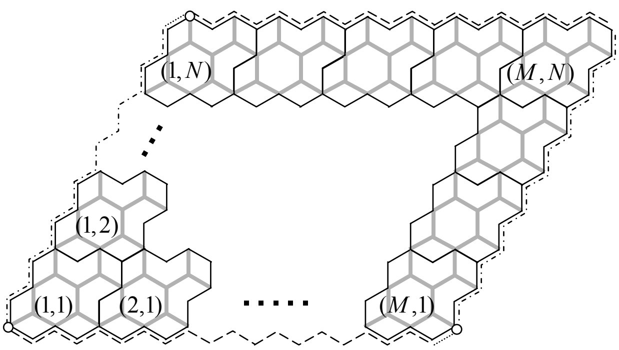

Fig. 1. Periodic unit *kY* consisting of $M \times N$ subunits, each of which is an aggregate of 2×2 cells; chain, dashed and dotted lines indicate three pairs of boundary sides, and small circles designate the nodal points with $\dot{u}_i^* = 0$.

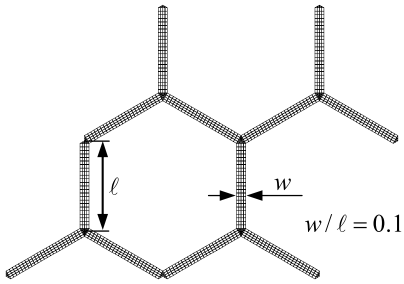

Fig. 2. Shape and finite element mesh of subunits (1296 elements, 1598 nodes).

Analysis of Honeycombs

The theory mentioned above was applied to the in-plane buckling analysis of an elastoplastic honeycomb. The honeycomb was subject to in-plane either uniaxial or equi-biaxial compression. We employed the periodic unit kY that consisted of $M \times N$ subunits, each of which was an aggregate of 2×2 cells (Fig. 1). This type of periodic units are denoted as $Y_{2M\times 2N}$. Figure 2 depicts the shape and finite element mesh of subunits employed in the present study. The thickness and length of cell walls, w and ℓ, have a ratio of $w/\ell = 0.1$, as shown in the figure. The mesh was formed by means of four-noded isoparametric elements. Each node had three nodal values to represent the generalized 2D deformation in which $\dot{u}_3^* \neq 0$ but $\partial \dot{u}_i^* / \partial x_3 = 0$, $i = 1, 2, 3$.

The analysis of uniaxial compression was done by use of the $Y_{2\times 2N}$ type of periodic units. Then, subsequent to the first bifurcation that was simple and had a short wavelength, the second bifurcation occurred in macroscopically unstable states (Fig. 3). The second bifurcation had the following features: It was double, i.e., $m = 2$, in contrast to the first bifurcation. It occurred earlier with the increase of the vertical cell number, but $Y_{2\times 16}$, $Y_{2\times 32}$, and so on had almost the same second bifurcation points, as indicated in Fig. 3. Therefore, we can say that the vertical cell number of the periodic unit has significant influence on the second bifurcation under uniaxial compression.

The finding of $m = 2$ mentioned above suggested two basic eigenmodes $\phi^{(1)}$ and $\phi^{(2)}$ at the second bifurcation points. The inverse power method, then, allowed us to determine combined eigenmodes of the second bifurcation, which are expressed as $\phi = c^{(1)}\phi^{(1)} + c^{(2)}\phi^{(2)}$. Here $c^{(1)}$ and $c^{(2)}$ are constants. We thus found that the second bifurcation has the Bloch wave property. The wave property can provide the eigenmode ϕ with a phase shift in addition to the wave form. This additional degree of freedom accounts for $m = 2$ at the second bifurcation points under uniaxial compression.

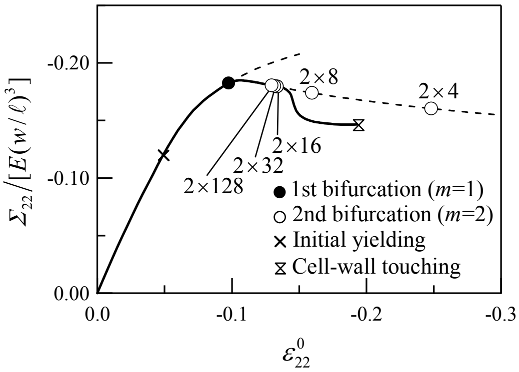

Fig. 3. Macroscopic stress-strain relation under uniaxial compression.

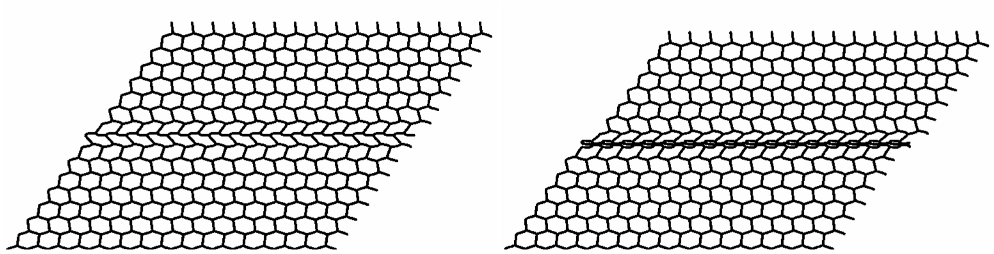

(a) (b)

Fig. 4. Microscopic deformation of $Y_{2\times16}$ under uniaxial compression; (a) $\varepsilon_{22}^0 = -0.15$, (b) $\varepsilon_{22}^0 = -0.19$.

The second post-bifurcation analysis was performed by adding a basic eigenmode $\boldsymbol{\phi}^{(1)}$ to the fundamental solution. The addition of $\boldsymbol{\phi}^{(1)}$ did not instantly influence on the change in macroscopic stress in accordance with orthogonality (2), but shortly after the second bifurcation point, macroscopic softening became significant temporarily and then calm, as shown in Fig. 3. The development of microscopic deformation after the onset of the second bifurcation is illustrated in Figs. 4(a) and 4(b), in each of which the configuration of $Y_{2\times16}$ at a macroscopic strain is arranged periodically in the x_1-direction. It is seen from the figures that microscopic buckling localized in a cell row perpendicular to the loading direction with the increase of macroscopic compressive strain.

The buckling behavior under equi-biaxial compression was analyzed by use of the $Y_{2N\times2N}$ type of periodic units. Then, as was demonstrated in [3, 4], a triple bifurcation appeared to cause the flower-like buckling mode, which was experimentally found in [2]. Subsequently, a long-wave, sextuple bifurcation occurred soon after initial yielding, if such large periodic units as $Y_{14\times14}$, $Y_{16\times16}$, and so on were assumed (Fig. 5). Let us emphasize that the second bifurcation was sextuple, i.e., $m = 6$, in the case of equi-biaxial compression. This multiplicity was interpreted by noticing that the three directions of cell walls are equivalent under equi-biaxial compression, and that long-wave eigenmodes have the multiplicity of $m = 2$ due to the additional degree of freedom resulting from phase shifts. The sextuple bifurcation was, thus, ascribed to synchronicity of the three long-wave eigenmodes inducing the localization of microscopic buckling in cell-rows perpendicular to the three directions of cell walls.

The second bifurcation under equi-biaxial compression, which turned out to be asymmetric, induced some enhancement of macroscopic softening shortly after the second bifurcation point, as shown in Fig. 5. The microscopic deformation caused by the second bifurcation is depicted in Figs. 6(a) and 6(b). It is seen from the figures that the flower-like buckling mode uniformly prevailed at the second bifurcation point, and that the localization of microscopic buckling developed in deltaic regions. The localization in such unnarrow regions was likely to occur experimentally [2]. Incidentally, changing the sign of the eigenmode at the second bifurcation point resulted in jerky variations in macroscopic stresses.

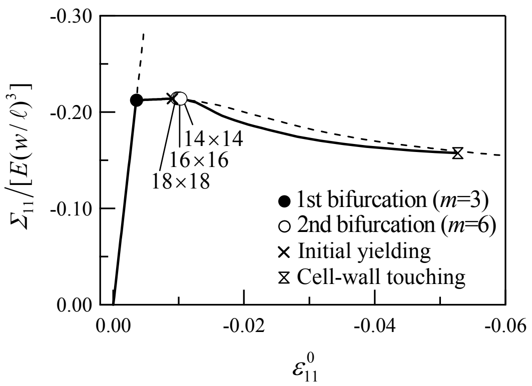

Fig. 5. Macroscopic stress-strain relation under equi-biaxial compression.

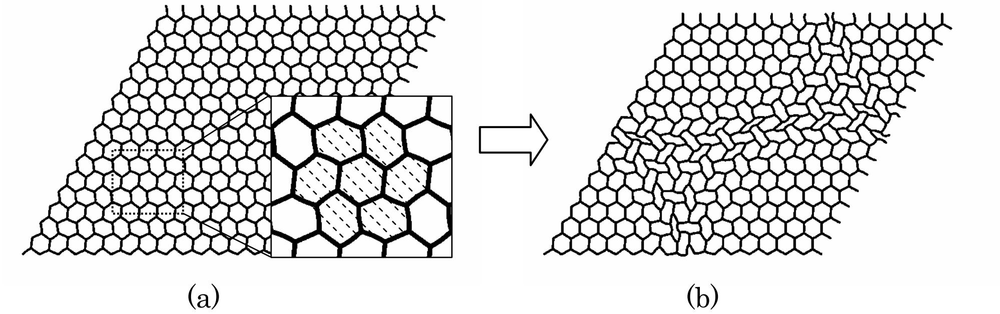

Fig. 6. Change in deformation of $Y_{16\times16}$ due to the second bifurcation under equi-biaxial compression; (a) second bifurcation point, (b) $\varepsilon_{11}^0 = \varepsilon_{22}^0 = -0.04$.

Conclusions

On the basis of a two-scale theory of the up-dated Lagrangian type, a general framework was developed to analyze microscopic bifurcation and post-bifurcation behavior of elastoplastic, periodic cellular solids. The framework was applied to the in-plane buckling analysis of honeycombs. We thus had the following findings: Subsequent to the microscopic bifurcation with no dependence on periodic length, the long-wave microscopic bifurcation depending on periodic length occurred in macroscopically unstable states. In the case of equi-biaxial compression, the flower-like buckling mode having occurred in a macroscopically stable state changed into an asymmetric, long-wave mode due to the sextuple bifurcation in a macroscopically unstable state, leading to the localization of microscopic buckling in deltaic areas.

References

1 Gibson, L.J. and Ashby, M.F. (1997): *Cellular Solids, Structure and Properties, 2nd Edition*. Cambridge University Press.

2 Papka, S.D. and Kyriakides, S. (1999): "Biaxial Crushing of Honeycombs – Part I: Experiments". *Int. J. Solids Struct.,* Vol. 36, pp. 4367-4396.

3 Ohno, N., Okumura, D. and Noguchi, H. (2002): "Microscopic Symmetric Bifurcation Condition of Cellular Solids Based on a Homogenization Theory of Finite Deformation". *J. Mech. Phys. Solids,* Vol. 50, pp. 1125-1153.

4 Okumura, D., Ohno, N. and Noguchi, H. (2002): "Post-Buckling Analysis of Elastic Honeycombs Subject to In-Plane Biaxial Compression. *Int. J. Solids Struct.,* Vol. 39, pp. 3487-3503.